DOI: 10.13009/EUCASS2019-421

8TH EUROPEAN CONFERENCE FOR AERONAUTICS AND AEROSPACE SCIENCES (EUCASS)

DOI: ADD DOINUMBER HERE

Reusable stage concepts design tool

Lars Pepermans⋆, *Barry Zandbergen*†
⋆*Delft University of Technology*
Kluyverweg 1, 2629 HS Delft
lpepermans@outlook.com
†*Delft University of Technology*
Kluyverweg 1, 2629 HS Delft

Abstract

Reusable launch vehicles hold the promise of substantially reducing the cost of access to space. Many different approaches towards realising a reusable rocket exist or are being proposed. This work focuses on the use of an optimisation method for conceptual design of non-winged reusable upper stages, thereby allowing it to take into account landing on land, sea or mid-air retrieval as well as landing the full stage or the engine only.

As the optimisation criterion, the ratio of the specific launch cost of the reusable to the expendable version is used. The tool also provides for a Monte Carlo analysis, which allows for investigating the ruggedness of the design solution(s) found.

The article will describe the methods implemented in the Conceptual Reusability Design Tool (CRDT) together with the modifications made to ParSim v3, a simulation tool by Delft Aerospace Rocket Engineering. Furthermore, it will present the steps taken to verify and validate CRDT. Finally, several example cases are presented based on the Atlas V-Centaur launch vehicle. The cases demonstrate the tools capability of finding optimum and the sensitivity of the found optimum. However, it also shows the optimum when the user disables some Entry Descent and Landing (EDL) options.

1. Introduction

To make space more accessible, one can reduce the cost of an orbital launch. Of the total cost per launch, the manufacturing cost of the rocket makes up 60% and 70%.[10] To reduce the manufacturing costs, one can consider designing a reusable rocket stage. This will reduce the hardware costs but at the expense of higher development cost. Both SpaceX and United Launch Alliance have added reusability to their launcher's first stage to decrease the cost per launch. Besides that, several other companies are investigating reusing the first stage. Most research focuses on the first stage and very little research is done on the upper stage. The upper stage of the Atlas V Centaur launcher is about 25% of the mass and 30% of the hardware cost of the entire launcher.[23] This means that a significant portion of the cost is not considered for reuse at the moment. Upper stage reusability has been proposed for the Blue Origin New Glenn rocket[3] and the Kistler K1 rocket.[6] However, neither have proven this in flight. The USA Space Shuttle is the only example of an operational reusable upper stage.

From literature, two classes of entry vehicles can be identified: ballistic or lift generating vehicles.[31] Most research done on the upper stages focuses on the winged entry vehicles following a glide entry, such as the USA space shuttle, SpaceX BFR, and CNES/ESA Hermes.[15] This means that the stage has to be developed from scratch. The development of an entirely new stage, however, is a time and cost-intensive process. Therefore the focus of this research is on making an existing upper stage reusable by applying commercially available entry descent and landing (EDL) hardware.

For this research, it is assumed that the stage performs a ballistic entry and that no form of a winged entry vehicle is possible. It furthermore assumes that the initial condition for the stage is a stable orbit, this orbit is the target orbit for the satellite.

When adding reusability to a stage, one adds hardware to bring it back the stage safely to the ground. This added hardware comes at a price in terms of payload reduction and hardware cost increase. Besides that, reliability might decrease when a stage is reused often. To determine whether the reusable upper stage is cheaper than an expendable upper stage, the Reuse Index as proposed by United Launch Alliance (ULA), is used.[23] An overview of the investigated hardware and the Reuse Index can be found in section 2. As the Reuse Index requires the cost and mass for each

Copyright © 2019 by L. Pepermans and B.T.C Zandbergen. Published by the EUCASS association with permission.

DOI: 10.13009/EUCASS2019-421

recovery element of hardware required. These modifications to the stage are represented in an ID. Together with the various mass and cost models, this is shown in section 4.

To determine whether a solution exists that can reduce an upper stage cost's by adding reusability, an optimisation tool has been developed. The optimisation tool is based upon a genetic algorithm and is described in section 3. This method has been chosen due to the non-linear and non-continuous nature of the problem. When an optimum has been found, the tool performs a Monte Carlo analysis to determine the sensitivity of the found solution.

The individual mass and cost models have all been verified using existing information. The trajectory verification, together with the verification of the optimisation algorithm, is done in section 5.

Finally, in section 6, a case study is done using the Centaur upper stage. This case demonstrates the feasibility of upper stage reusability and shows the capabilities of the tool. The conclusions can be found in section 7.

2. Background

From literature, it was found that the flight of an upper stage consists of five main phases, see Figure 1. Each phase requires the addition of hardware elements, these are presented in in Table 1. Figure 1 is preceded by the ascent flight of the upper stage and is followed by the retrieval and refurbishment of the upper stage.

Figure 1: Flight phases of a reusable upper stage

Table 1: Overview of identification phases in the reusable flight

Phase	**Design options**
1) De-orbit	Two burn de-orbit
2) Atmospheric entry	Conventional heat shield Inflatable heat shield
3) Descent	Ballute Supersonic parachute Subsonic parachute Drag plate Engine burns Rotor landing
4) Landing	None Airbag Retrorocket Water landing Mid air recovery
5) Retrieval and Refurbishment	

The de-orbit phase is done using a Hohmann transfer orbit with two engine burns, one at the apogee of the initial orbit, and one at the user-defined entry point (periapsis), see Figure 2. The entry point is defined by its altitude [m], velocity [m/s] and entry angle [deg] [1]. The goal of the first burn is to attain the desired entry altitude while the second determines the entry angle and entry velocity.

[1]Downward from local horizon is negative

DOI: 10.13009/EUCASS2019-421

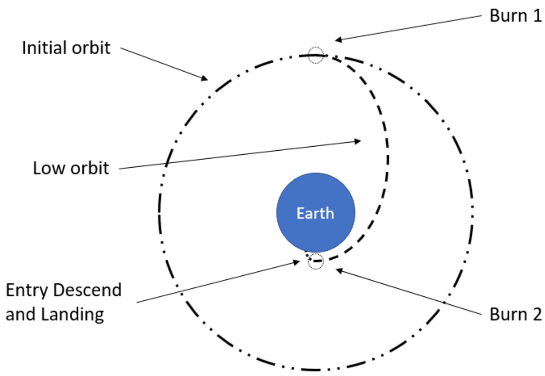

Figure 2: De-orbit manoeuvres

When re-entering the atmosphere, the stage experiences heat transfer due to aerothermal heating. This resulting heat flow can require the use of thermal protection system is. Literature suggests two options for thermal protection: solid heat shields and inflatable heat shields. The solid heat shield is however a more conventional solution the inflatable heat shield has the advantage that it can combine the functions of thermal protection, parachute, and airbag landing system.[8,14] It has however a lower technology readiness level compared to the conventional heat shields.

To ensure a safe landing, one or more decelerators are required. Four main decelerator options have been identified from literature: parachutes, drag plates, engine burns, and rotor landing. Even though the rotor landing nicely combines the decelerator and landing options, the technology readiness level is not sufficient for current applications and thus not considered.[22]

The parachutes identified to be of use for this research are ballistic, non-steerable parachutes. The parachutes considered for this research come in three categories: ballute, ribbon parachutes, and Ringsails parachutes. The ballute's primary function is stabilisation of the stage and is used when the upper stage is unstable during the flight. The ribbon parachutes are assumed to be supersonic, drogue parachutes where the Ringsail parachutes are mainly used for subsonic, main parachutes.[12] The choice of parachutes is based upon the deployment altitude:

- 100000 m - 60000 m - Ballute
- 60000 m - 7500 m - Ribbon parachute
- 7500 m - 0 m - Ringsail

The drag plates are deployable, solid drag enhancement surfaces. These surfaces increase the drag of the body to decrease the terminal velocity. Drag plates can also provide aerodynamic control, although this is not considered in this research.

Engine burns are an air-independent method of deceleration. This means it can decrease the maximum dynamic pressure and heat flux on the stage during the atmospheric entry flight. When a concept separates the engines and propellant tanks, engine burns are not a feasible decelerator.

The landing hardware assumes that the stage always performs a safe landing as long as the terminal velocity of the stage is within the allowable range. Four landing options have been identified from literature: retrorockets, airbags, water landing and mid-air retrieval.[12]

Both the retrorockets and airbags are used for a dry landing; this can either be on land or a ship. The retrorocket solution equips the stage with small solid rocket engines that are fired just before the stage hits the ground. The advantage of this system is that the maximum allowable terminal velocity is assumed to be 100 m/s. The airbag system has a lower maximum acceptable landing velocity of 10 m/s.[12] However, it has a lower cost than the retrorocket system for landing velocities below 12 m/s. During a land landing, the stage is retrieved by a truck with a crane. This is comparable to the Soyuz landings.

When the stage lands in the water, it is assumed that any landing is safe when the landing velocity is below 20 m/s. This is comparable to the proposed splashdown velocity of the Ariane 5 boosters.[30] The added mass and cost comes from the flotation devices required to keep the stage afloat and protect the engine against salt water. For a water landing the stage is retrieved using a ship, comparable to the SpaceX Dragon capsule.

During a mid-air retrieval, the stage is intercepted in flight by a helicopter.[16] This means no additional hardware is required for landing. It only imposes the requirements that the final decelerator stage is a parachute system.

DOI: 10.13009/EUCASS2019-421

The last step of a reusable stage, is that it needs to be refurbished for re-flight. SpaceX suggests that the refurbishment of a rocket stage is done in three steps.[2] These are as follows:

1. Replace broken/discarded elements
2. Inspection
3. One full engine burn as flight acceptance

An important figure of merit in this respect is the Reuse Index defined by United Launch Alliance (ULA).[23] The Reuse Index divides the cost per kilogram of the reusable version by the cost per kilogram of the expendable version. When this Reuse Index is below 1, the reusable alternative is cheaper. For optimisation, the Reuse Index is minimised.

3. Tool

The tool, written in MATLAB, allows for rapid mass and cost estimations of the reusable upper stage. The tool is set up to be highly modular, allowing the implementation of new different stage configurations and mass/cost modules. Mass and cost models allow calculating the cost and mass needed to determine the inputs for the Reuse Index. These modules are free to be updated during further development of the tool. CRDT has two main modes of operation: optimisation and sensitivity analysis. Both are explained in subsection 3.1 and subsection 3.2.

A simplified flow diagram of CRDT can be found in Figure 3. The optimisation algorithm chosen for the tool is a genetic optimisation algorithm as the non-linear and non-continuous behaviour of the optimisation function. For the sensitivity, the tool has a Monte Carlo analysis.

All trajectories and dynamics are calculated using a modified version of the ParSim v3 simulation tool developed by the Parachute Research Group (PRG) of Delft Aerospace Rocket Engineering (DARE). When ParSim performs the trajectories calculations, it adds the mass and cost of the extra hardware using the models described in section 4. Parsim V3, and therefore CRDT, uses a 2D, non-rotating, round earth model. Furthermore, the atmospheric model is the COESA Atmosphere Model, which comes standard in MATLAB. The aerothermal heating is based upon previous work by Brandis et all.[5]

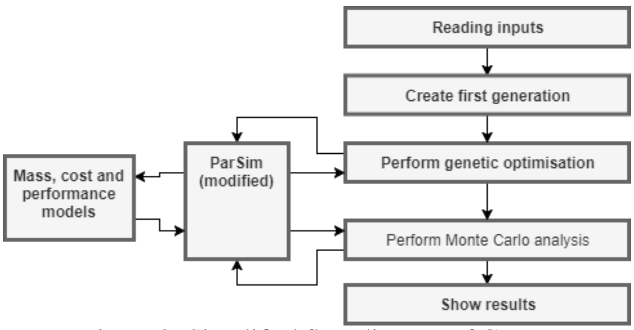

Figure 3: Simplified flow diagram of CRDT

The mass of the EDL hardware is added before the trajectory calculations of the stage. This added mass is subtracted 1-on-1 from the payload capacity of the stage. The costs are divided into reusable EDL hardware and non-reusable EDL hardware.

3.1 Optimisation

A genetic optimisation algorithm is chosen as the Reuse Index is non-linear and non-continuous. The genetic optimisation transfers the best options to a new generation; these are called the elites. The remainder of the generation is filled up with children that are a recombination of the parent genes. After the generation is filled, random mutations are performed on the individual genes.

The tool allows for the addition of SuperElites and bees, as can be seen in Figure 4. The SuperElites are elites that are immune to mutations to allow for finding hard to find optima. This can be for a solution that is very close to a constraint or a narrow minimum. The bees can be used in the case where the tool gets stuck on a local minimum and are always taken as a percentage of the total killed genes. These additions can be useful for making calculations more efficient, but should not be used to frequently. It is advised to increase the number of genes, rather than adding bees or SuperElite.

DOI: 10.13009/EUCASS2019-421

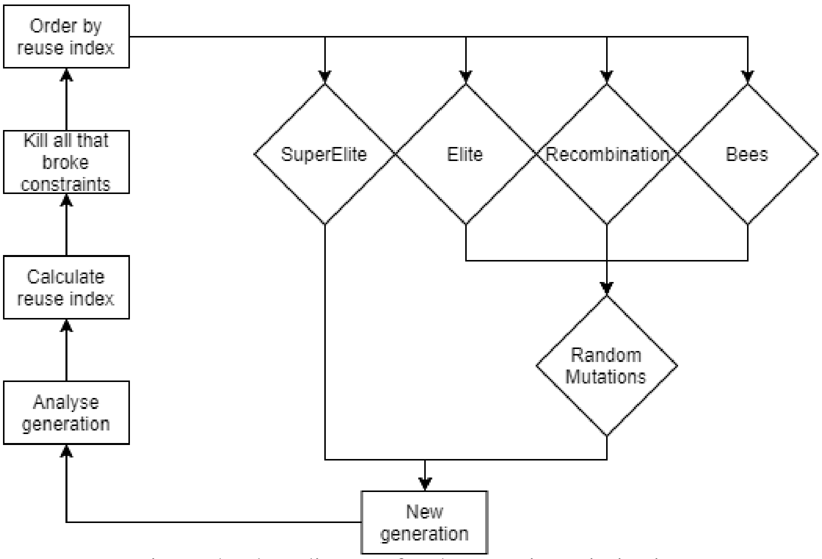

Figure 4: Flow diagram for the genetic optimisation

The optimisation is stopped when the minimum Reuse Index remains within 0.01 difference for three generations. Furthermore, the code has two additional criteria that can be used to trigger a stop. The first is when the maximum number of generations has been reached; this is triggered when a problem has no solution. The second is when the minimum Reuse Index increases, while the number of non zero genes decreases. A non zero gene is a gene that does not breach any of the user set constraints and is thus eligible for being a parent gene. A decrease in non zero genes can indicate a too low amount of genes. When this is triggered, the user is warned and has the option to continue the run still or abort the run.

A more detailed view of the CRDT block diagram is given in Figure 5. As can be seen, the tool repeats the block until the end condition is reached. When the optimisation is ended, it moves on to the Monte Carlo analysis. Otherwise, a new generation is created, and the loop continues.

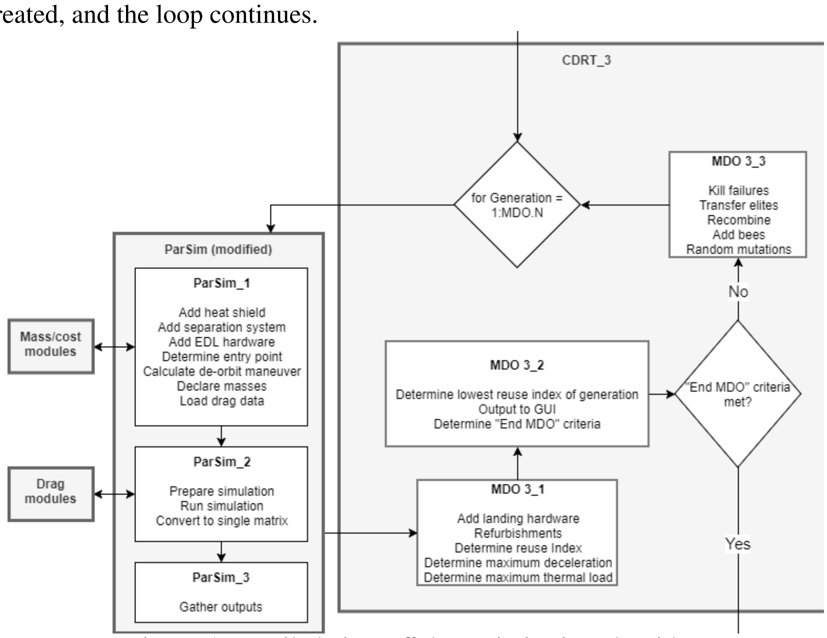

Figure 5: Detailed view off the optimisation algorithm

3.2 Sensitivity analysis

The sensitivity analysis is done by dividing the uncertainties into five categories, based upon the origin of the uncertainty. Table 2 shows the parameters effected per category.

1. Uncertainty in stage geometry
2. Trajectory uncertainty
3. Onboard State estimation
4. Uncertainty in construction, trajectory, and state estimation (all three above)

DOI: 10.13009/EUCASS2019-421

5. Uncertainty in mass and cost estimations

Each variation is assumed to be a normal distribution centred around the found optimum. The user is free to change the standard deviation for all inputs or put it to zero. The standard deviation is taken as a fraction of the mean. As an example, when the deployment altitude is set to 10,000 meters and the uncertainty is put to 0.2. The normal distribution parameters can be seen in Equation 1 and Equation 2.

$$\mu = 10000 \quad (1) \qquad \sigma = 0.2 * 10000 \quad (2)$$

Table 2: Input for the sensitivity study

Parameter	**1**	**2**	**3**	**4**	**5**
Drag coefficient of all elements	x			x	
Initial stage mass	x			x	
Heat shield area	x			x	
Entry conditions		x		x	
Separation altitude			x	x	
Parachute deployment altitude			x	x	
Parachute area	x			x	
Drag plates deployment altitude			x	x	
Drag plate area		x		x	
Engine burn start altitude	x			x	
Engine burn time	x			x	
Engine throttle setting			x	x	
Individual mass/cost models					x

4. Models

The models used to estimate the performance, mass and cost of each of the hardware choices can be found in Table 3. The cost models are build up of the hardware cost and the manhour costs and are estimated based on experience or historical data. All models are either empirical or semi-empirical. Some models use a up bottom approach. This means a breakdown is made of the parts required, the mass and cost of these parts are estimated and summed up to determine the total mass and cost.

The development costs per element are estimated trough Transcost; this is shown in Equation 3, the factors f1 and f3 are taken from Koelle. The f1 factor represents the technological readiness of the hardware where the f3 factor represents the team experience.[13]

$$C_{total} = C_{hardware} * f1 * f3 \quad (3)$$

DOI: 10.13009/EUCASS2019-421

Table 3: Overview of Entry Descent and Landing (EDL) options implemented and their mass and cost models

Hardware		**How implemented in the dynamics model**	**Mass model**	**Cost model**
Separation system		-	Historic data[7,27–29]	Function of system mass
Thermal protection	Solid heat shield	-	Milos et all[8]	Milos et all[8]
	Inflatable heat shield	Change the frontal area of the stage to the area of the heat shield	Previous research[19,25]	Bottom up model
Decelerators	Parachute	EDL force superimposed on the body drag force	Knacke[12]	Bottom up model
	Drag plates		Bottom up model	Bottom up model, function of system mass
	Engine burn		Function of burn time	Function of propellant mass
Landing	Retrorockets	Prescribed safe landing	Knacke[12]	Bottom up function of retrorocket mass. Mass divided in propellant and casing
	Airbags		Knacke[12]	Bottom up function of airbag mass
	Flotation device		Bottom up model	Bottom up, function of system mass
	Mid air retrieval		None	None

4.1 Thermal Protection

The mass and cost of a solid heat shield originate from previous work.[8] The mass of the inflatable heat shield comes from previous missions and pre-existing mass models.[19,25] The mass estimation is a function of a constant multiplied with the area of the heat shield. From literature it can be seen that this constant is between 3 and 5 kg/m^2. Figure 6 shows these estimates as the dashed lines. The solid line indicates the average of 4 kg/m^2. The figure also shows the mass of three reference missions. These missions are IRDT, LOFTID, and HEART. Each mission is indicated with two asterisks in the plot, showing the total system mass and the mass of just the inflatable structure.[9,17,32]

Figure 6 shows the mass of the reference missions with and without inflation system. As can be seen, the references missions confirm the large uncertainty of the mass estimations. The area of the inflatable heat shield is set from once the frontal area of the initial stage, to a user defined maximum.

Cost estimations are done using a bottom-up approach, assuming the bag is made up of 40mm Nextel 440, 236mm Pyrogel3350, 1mm Kapton, and 5mm Kevlar.[24] For the solid heat shield, the verification can be found in Figure 7. This shows the model has been properly implemented into CRDT.

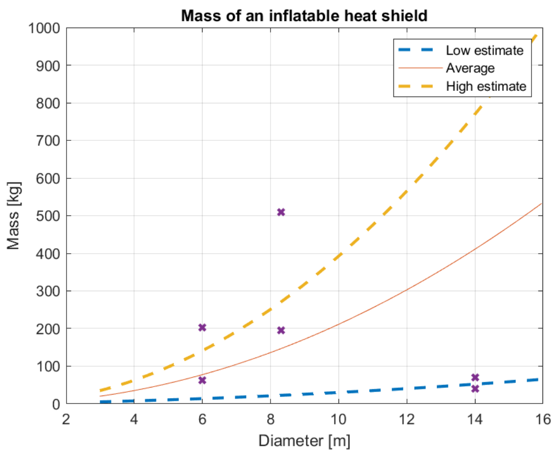

Figure 6: Mass verification of inflatable heat shield

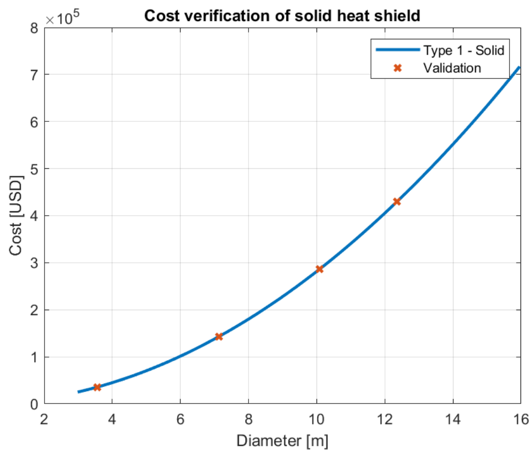

Figure 7: Cost verification of the solid heat shield

DOI: 10.13009/EUCASS2019-421

4.2 Decelerator hardware

The parachute mass models originate from empirical data for the ribbon and Ringsail parachutes.[12] For the ballute decelerator, the data originates from the historical data.[18,20] Here it can be seen that the models for the ribbon and Ringsail parachutes match nicely. However, the model of the ballute is no longer accurate below 5 meters diameter. For the Ringsail, the mass model is valid up to a diameter of 30 meters. The mass model of the ribbon parachute is valid up to 24.3 meters diameter.[12]

To verify the cost model, both parachute models are run with the same inputs. The same is done for the cost model, which proved to be a good match with the verification data.

The drag plate model is based upon the required plate area assumed it is made out of aluminium. The mass of the plate is multiplied by two to include the mass of the deployment systems. The drag plates are limited to an area between 1 and 5 m^2. When comparing the analytically calculated data with the model, one finds a perfect fit.

The engine burns in CDRT are modelled in two different ways. The de-orbit burns are a function of the required delta-v, where the deceleration burns are a function of the required burn time. The mass models are compared to analytical data, where the cost models are compared to one another.

The drag plate model has been verified for the range of 1 to 5 m^2. The engine burn models have been verified for a range of 1 through 20 delta-V and a burn time between 1 and 20 s. Over these ranges, it was verified that the models had been correctly implemented.

4.3 Landing hardware

Historical data was used to model the mass of the retrorocket and airbag systems.[12] For the water landing system, it is assumed that the bag needs to be large enough to keep the stage afloat. This flotation bag is assumed to be made out of Hypalon, which costs 68 British pounds per square meter and 1.3 kg per square meters.

The verification of the mass models was done with a landing velocity between 1 and 20 m/s. The retrorocket model verification was done up to 100 m/s, as the maximum terminal velocity was shown to be higher. For these ranges, it was demonstrated that the model had been implemented properly.

4.4 Retrieval and Refurbishments

The cost of retrieval depends on the landing location: water, land or mid-air retrieval. Based on this, a retrieval vehicle is chosen at a certain cost per year. The vehicle costs have been taken from earlier work performed at Delft University of Technology together with the NLR.[26] This cost is divided over the launches per year. The costs are added as a total cost divided over the number of flights per year. The cost of the refurbishments is estimated as a required number of man-hours. Furthermore, the rebuild of the stage is estimated as the fraction of the separated mass.

4.5 Stage Modifications

To accommodate for the additions to the stage, the user can opt to do one of four things as mentioned before.

For the Atlas V - Centaur upper stage it is quite well documented what the payload mass and launch cost for every version of the launcher is. For this modification, the type of launcher is changed to the variant with one more booster. For the configurations 431 and 551, this cannot be done as the Atlas V 441, and 561 does not exist in the current ULA inventory. Whenever an ID shows up, that does require a 441 or 561 configuration the solution is considered a lethal and thus killed.

The increased mass and cost of elongated tanks is determined by looking at historical data. This can be done as the Centaur stage has had quite some upgrades over its lifetime. Whenever both an extra booster and elongated tanks are required, the modifications are superimposed.

5. Tool Verification

The verification of the tool is done in two steps. First, the trajectory was compared by comparing the outputs of CRDT to the outputs of ParSim. Second CRDT was used to find multiple optima and analyse the behaviour. The verification of the individual models has been discussed in section 4.

5.1 Trajectory

Verification of the modified ParSim is done compared to ParSim v3 as published at the IAC2018.[21] The verification matrix can be seen in table 4. For all of the above cases, the difference in terms of altitude-time and velocity-time between CRDT and ParSim v3 was less than 5%. This can be attributed to changes made into the code to allow for faster calculations.

DOI: 10.13009/EUCASS2019-421

Table 4: Trajectory verification

Case	ParSim v3 input
Bare stage	Standard case for ParSim
inflatable heat shield	Increase the rocket diameter to the desired frontal area, whilst keeping the mass of the stage the same
Parachutes	Standard case for ParSim
Drag plates	CD modification of the stage at Mach = 3.0

5.2 Optimisation

When running the case for a Centaur-like stage in low earth orbit, one can find a solution. The inputs and results of the cases ran for verification can be found in section 6. Figure 8a and Figure 8b show the Reuse Index of both LEO cases over the generations. The same run has been done multiple times, always resulting in the same result.

It is not uncommon for the Reuse Index to jump up at some points. This can be seen in Figure 8a and Figure 8b. However, if the generation is sufficiently large, it will always return to a lower value for the optimisation function. As an extra help, CRDT plots the number of non zero genes together with the average Reuse Index of the generations as well. When the number of non zero genes goes up, and the average decreases, the user knows the optimisation algorithm is still progressing.

Taking these observations into account, it can be said that the optimisation algorithm can be considered verified.

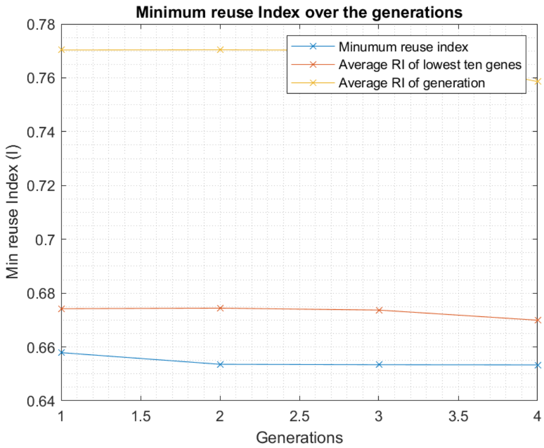

(a) Case 1

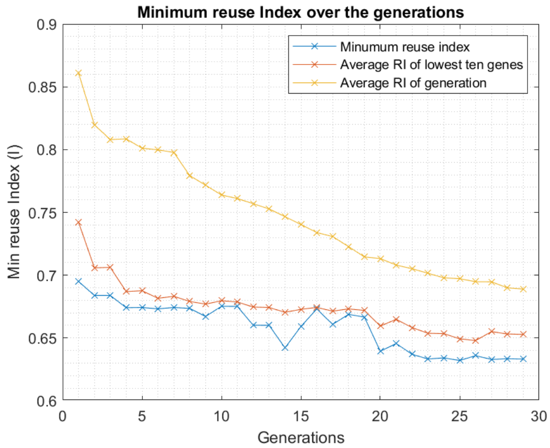

(b) Case 2

Figure 8: Lowest Reuse Index over generations for two CRDT runs

6. Example case

As a reference vehicle for this example, the Atlas V Centaur launcher has been used. This is done because:

- The Centaur stage is a relative lightweight stage with a dry mass of just over 2200 kg. This makes a recovery more easy as it reduces the loads on the stage.[4]
- The Centaur stage uses the relatively expensive (compared to the rest of the stage) RL-10 engine thus making reusability more interesting
- The RL-10 engines are restartable and throttleable thus making them more ideal for EDL manoeuvres as it allows for more precise manoeuvres[11]
- Reusability and landing capabilities of the RL-10 family has been demonstrated in the DC-X vehicle[1]

Furthermore, as the Centaur stage has gone through many iterations over the years, it is possible to make estimates as to how heavy and expensive an elongated centaur stage would be. The inputs used for the example cases can be seen in Table 5 and the constraints imposed on the stage can be found in Table 6.

Three cases are run coming from two orbits. The first two cases are the low earth orbit (LEO) case, and the third is the Geostationary transfer orbit (GTO) case. These inputs can be seen in Table 7. For the various cases, a sensitivity analysis is done demonstrating the stability of the found solution and the working of the tool.

DOI: 10.13009/EUCASS2019-421

Table 5: Centaur stage inputs

Parameter	Unit	Value
Initial Mass (empty)	kg	2247
Mass post separation	kg	561.75
Diameter	m	3.05
Length	m	12.68
Thrust Vac 100%	N	99200
Isp vacuum	s	462
Ae	m^2	3.63
Pc	MPa	4.41
Expansion ratio	-	88.1
Min throttle setting	fraction	0.75
OF ratio	-	5.88
Mass fraction	fraction	0.25
Cost	M $	20
Cost engine	Percentage	80
Nr yearly flights	Nr	10
Nr of reuses	-	15

Table 6: Centaur stage Constraints

Parameter	Unit	Value
Acceleration	m/s^2	1000
Landing velocity Nothing	m/s	5
Landing velocity Airbag	m/s	20
Landing velocity Retrorocket	m/s	100
Landing velocity Water	m/s	20
Landing velocity MAR	m/s	50
Max payload reduction factor (p)	-	3

Table 7: Inputs for the LEO and GTO cases

Case	LEO	GTO
Initial orbit	400	XX
Allowable heat shield hardware	All	Inflatable
Allowable decelerator hardware	All	Parachutes
Allowable landing hardware	Retrorocket and airbag	Retrorocket and airbag
Allowable modifications	Extra booster	Extra booster
Separation	Allowed	Allowed
Nr of reuses	15	15
Nr of genes	2000	2000
Nr of elites	0.2	0.2
Nr of SuperElites	0	0
Nr of mutations of genes	0.5	0.5
Nr of mutations in genes	0.2	0.2
Nr of bees	0	0

For the cases as described here, CRDT is capable of determining the Reuse Index of one generation between 10 and 15 minutes, depending on the number of genes. This leads to a total computing time of below two hours for these two runs. All runs have been done on a typical consumer's high-end laptop.

6.1 LEO case with retrorockets

When running the LEO case with all EDL options, one finds a solution using an inflatable heat shield and retrorockets for landing. The heat shield area of 12.3 m^2 is found. Due to the large size of the inflatable heat shield and the high allowable landing velocity of retrorockets, no deceleration hardware is required.

After 15 re-flights, the stage reaches a Reuse Index 0.655. The found solution has a Reuse Index of 1.5 for a single flight, and the Reuse Index reaches below one after three flights. The system is required to add an estimate of 544 kg of extra hardware, of which about half is propellants. With a total cost estimated at 47919 USD for reusable recovery hardware and 7807500 USD for non-reusable recovery hardware. This added mass leads to a performance reduction of only 5 percent.

DOI: 10.13009/EUCASS2019-421

Table 8: Mass comparison of the LEO case

Case	Mass Case[kg]	Cost [USD]
Total added	544	$C(RHW) = 47919$ $C(RR) = 7807500$
Propellants [%]	53	1
Heat shield [%]	7	81
Separation system [%]	4	7
Parachute system [%]	0	0
Landing system [%]	36	11

When varying the initial Centaur empty mass between 1500 kg and 3000 kg, one can get insight into how the Reuse Index behaves for different stage masses. These results can be found in Figure 10. It can be seen that with lower stage mass, the Reuse Index decreases. This is expected as the landing hardware scales with the stage mass.

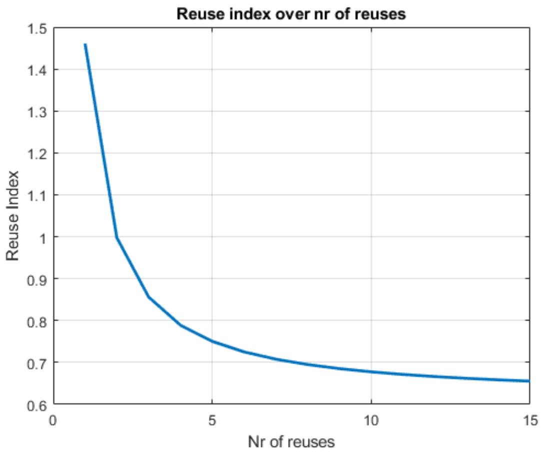

Figure 9: Reuse Index over nr of reuses

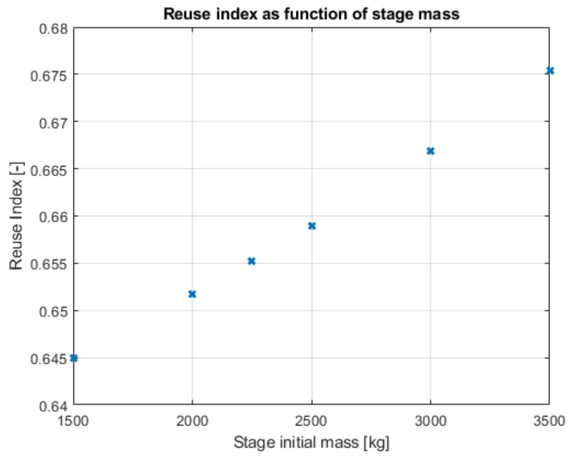

Figure 10: Reuse Index as function of empty mass

The uncertainties introduced onto the found solutions are 0.2 on all parameters. This means that all mass and cost models have a normal distribution were sigma equals 20% of the initial value. The numbering convention introduced in subsection 3.1 is used to indicate which uncertainty is which plot. For the final results published in the thesis, a more accurate uncertainty range is chosen. The Monte Carlo run was done using 1500 variations per run. The case demonstrated below is LEO case with a longer turnaround time. This increase the amount of manhours, thus increases the cost and increases the reuse index.

As can be seen in Figure 11, the Reuse Index is strongly influenced by the trajectory imperfections (boxplot 2). This is expected as the mass model for the inflatable heat shield is a function of the maximum dynamic pressure. As can be seen, this mainly negatively impacts the Reuse Index); the same results can be found in the combination plot (boxplot 4). As the mass and cost uncertainties are normally distributed, the Reuse Index can be brought down in the case when both the inflatable heat shield and the retrorocket models are less heavy and expensive than expected.

From the results, it can be seen that, with a sigma of 0.2 times the found value, the solution is quite robust. All variants in the box have a Reuse Index below 1, and even the whiskers of the plot remain below 1. Only for the trajectory imperfections and the mass/cost models, some outliers can be seen to breach the upper limit of 1 and are thus no longer more cost-effective.

DOI: 10.13009/EUCASS2019-421

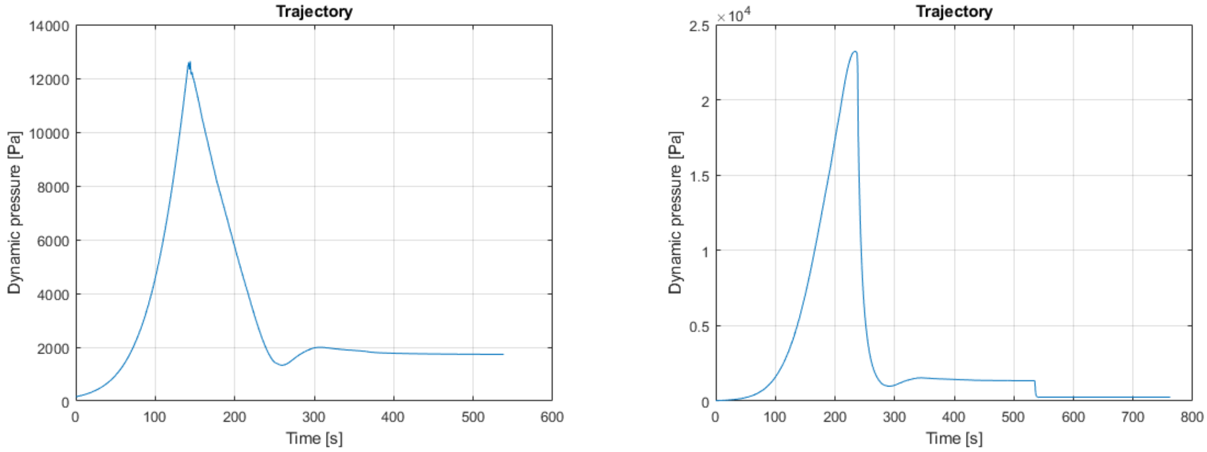

(a) Retrorocket landing (b) Airbag landing

Figure 12: Dynamic pressure plot for both solutions

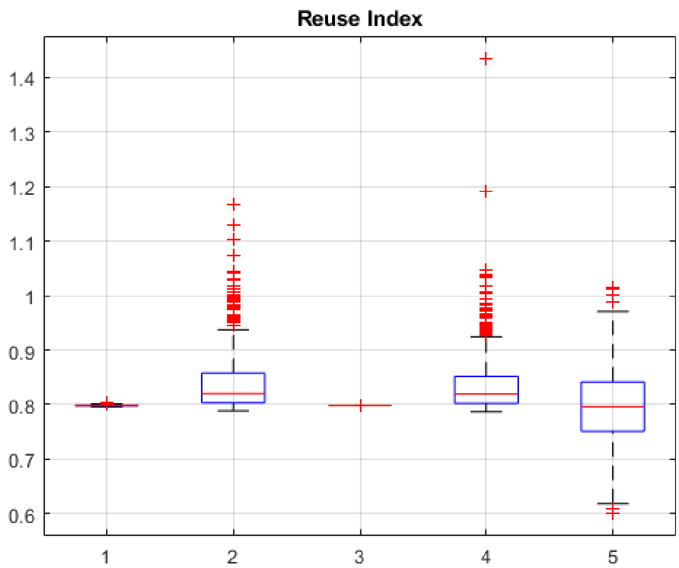

Figure 11: Uncertainty results - Reuse Index

6.2 LEO with airbags

When only selecting the airbag option, one finds a solution that requires a parachute for extra deceleration. This is due to the constraints mentioned in Table 6 where the airbag system is only capable of handling a 20 m/s or less impact. The dynamic pressure plots nicely show the effect of the parachute as the dynamic pressure in Figure 12b drops after 520 seconds, where the dynamic pressure in Figure 12b remains constant.

6.3 GTO

When running the solution found for the LEO case from GTO, one finds a Reuse Index of 0.944 after 15 flights. Furthermore, it can be seen that the stage does not breach constraints and is thus a feasible solution.

However, when running the GTO case described in Table 7, one can find a solution using an inflatable heat shield and retrorockets that has a Reuse Index of 0.72 after 15 reuses. The EDL hardware used in the GTO case is identical to the hardware used in the LEO case. However, the entry conditions have changed. This indicates that a single configuration can operate from both LEO can GTO.

DOI: 10.13009/EUCASS2019-421

7. Conclusion and Recommendations

It can be concluded that upper stage reusability is a potential method of hardware cost reduction. Given that the engine section of the stage has limits that are much more lenient than the entire stage, it is always advised to separate the upper stage. This design choice means that landing on the main engine is not feasible. Given that drag plates are relatively heavy, parachutes are the preferred decelerator option for the reusable upper stage. For the landing phase, one can select either an airbag or (solid propellant) retrorocket system. A water landing is not preferred as salt water strongly increases the refurbishment costs. The Mid-Air Retrieval option is feasible when the operating company has the capabilities to perform the operations. From, the optimisation runs, one can see that the retrorockets are always preferred over an airbag landing due to their overall lower mass and cost. Finally, it can be seen that the solution always converges to an inflatable heat shield with a maximum allowable area.
As the manhour cost is the most significant contribution to the cost factor, it also introduces the most substantial uncertainty into the solution. It is advised to take a good look into the manhour models and improve the models.
Besides focusing on better estimates of the manhour required for each operation, it is crucial to focus on the individual mass and cost models themselves. As more information becomes available on, for instance, the inflatable heat shield, the accuracy of these models can be increased.
One should also keep in mind that the upper stage is between 25 and 30 percent of the total hardware cost of the reference launcher. A Reuse Index between 0.7 and 0.75 can be found for most cases; this means that the overall reduction of hardware cost of 6 and 9 percent. Therefore, it is strongly advised to see upper stage reusability as an addition to first stage reusability and not as the sole method of cost reduction.

Furthermore, it can be concluded that a tool can be developed in MATLAB that can quickly run a feasibility and sensitivity study on reusable upper stages. This gives engineers the ability to perform a design study within a shorter time. It is recommended to expand the tool to allow suborbital trajectories to simulate the first stage or boosters as well. CRDT can be made available upon request for interested people to investigate and expand the possibilities.

The authors do advice an upgraded version of CRDT, which includes the uncertainty of the found solution in the optimisation tool. This allows for better inclusion of the uncertainty of an individual model when finding the optimum. In further work, it is recommended to take the reusability for the various EDL elements into account as the current equation assumes the lifespan of the EDL hardware is equal to the stage lifetime. Furthermore, it is recommended to take the ascent loads into account when investigating whether a solution breaks constraints.

Acknowledgements

The authors would like to thank M. (Mark) Rozemeijer for his work on ParSim V3 and Dr.ir. D. (Dominic) Dirkx for his assistance in the verification and validation of ParSim V3.

References

[1] Dc-x. http://www.astronautix.com/d/dc-x.html, 2017. 2019-03-20.

[2] Debating reusability. http://www.thespacereview.com/article/3583/1, 2018. 2019-06-18.

[3] Blue origin studying repurposing of new glenn upper stages, 2019. https://spacenews.com/blue-origin-studying-repurposing-of-new-glenn-upper-stages/, [2019-06-11].

[4] United Launch Alliance. Atlas V Launch Services Users Guide, 2010.

[5] A.M. Brandis and C.O. Johnson. Characterisation of stagnation-point heat flux for earth entry. *AIAA 45th AIAA Plasmadynamics and Lasers Conference*, 2014.

[6] Kistler Aerospace Corporation. K-1 vehicle payload users guide, 2001.

[7] Sierra Nevada Corporation. Space Technologies, Product Catalog, 2015.

[8] F. S. Milos D. J. Rasky and T. H. Squire. Thermal protection system materials and costs for future reusable launch vehicles. *Journal of Spacecraft and Rockets*, 38, 2011.

[9] R. A. Dillman, J. M. DiNonno, R. J. Bodkin, S. J. Hughes, F. M. Cheatwood, H. Blakeley, R. L. Akamine, and A. Bowes. Planned orbital flight test of a 6m hiad. Presented as the 2018 International Planetary Probe Workshop, Boulder, Colorado, 2018.

[10] N. G. Drenthe. Solstice - small orbital launch systems a tentative initial cost estimate, 2016.

DOI: 10.13009/EUCASS2019-421

[11] V.J. Giuliano. Cece: A deep throttling demonstrator cryogenic engine for nasa's lunar lander. *43rd AIAA/ASME/SAE/ASEE Joint Propulsion Conference & Exhibit*, 2007.

[12] T.W. Knacke. *Parachute Recovery System Design Manual*. Para Publishing, 1992.

[13] D. E. Koelle. The transcost-model for launch vehicle cost estimations and it's application to future system analysis. *Acta Astronautica*, 11, 1984.

[14] Vennemann U Anschuetz S Walther C Stelter K. Pitchkhadze L. Marraffa, D. Irdt - inflatable re-entry and descent technology. *Hot Structures and Thermal Protection Systems for Space Vehicles*, 2003.

[15] L. van den Abeelen. *Hermes, Europe's dream of independent manned spaceflight*. 2017.

[16] F. Zegler B. Mosley M. Gravlee, B. Kutter. Partial rocket reuse using mid-air recovery. *AIAA SPACE 2008 Conference & Exposition*, 2008.

[17] L. Marraffa, D. Kassing, P. Baglioni, D. Wilde, S. Walther, K. Pitchkhadze, and V. Finchenko. Inflatable re-entry technologies: Flight demonstration and future prospects, 2000.

[18] K. L. Miller, D. Gulick, J. Lewist, B. Trochman, J. Stein, D. T. Lyons, and R. G. Wilmoth. Trailing ballute aerocapture: Concept and feasibility assessment. *39th AIAA/ASME/SAE/ASEE Joint Propulsion Conference and Exhibit, Joint Propulsion Conferences*, 2003.

[19] NASA. NASA Technology Roadmaps. TA 9: Entry Descent and Landing Systems, 2015.

[20] A. Witkowski P. Woodruff, C. Yanaros. Low density supersonic decelerator ballute design and packing. *23rd AIAA Aerodynamic Decelerator Systems Technology Conference*, 2015.

[21] L. Pepermans, M. Rozemeijer, R. Gurumoorthy, Menting E, N. Suard, S. Khurana, T. Britting, and M. Serman. Flight simulations of the stratos iii parachute recovery system. *IAC-18*, 2018.

[22] R.A. Diaz-Silvia, M.M.Sarigul-Klijn, N Sarigul-Klijn. Rotary decelerators for spacecraft: Historical review and simulation results. *IAAA Space Forum*, 2013.

[23] M. M. Regab. Launch vehicle recovery and reuse. *AIAA SPACE 2015 Conference and Exposition*, 2015.

[24] R. A. Dillman H. S. Wright J. A. DelCorso S. J. Hughes, Dr. F. McNeil Cheatwood. Hypersonic inflatable aerodynamic decelerator (hiad) technology development overview. *AIAA 21st Aerodynamic Decelerator Systems Technology conference*, 2011.

[25] J. A. Samareh. Estimating mass of inflatable aerodynamic decelerators using dimensionless parameters. 2011.

[26] M. Snijder. Cost effectivness of the first stage recovery of a small satellite launcher, 2017.

[27] RUAG Space. PAS 381S (15") Separation System.

[28] RUAG Space. PAS 610S (24") Separation System.

[29] RUAG Space. Payload Adapter Systems for EELV.

[30] A. Vishnyak. Parachute simulations for ariane-5 booster recovery system design. *13th Aerodynamic Decelerator Systems Technology Conference, Aerodynamic Decelerator Systems Technology Conferences*, 1995.

[31] W. L. Hankey. *Re-Entry Aerodynamics*. 1988.

[32] H. Wright, A. Cutright, J. Corliss, W. Bruce, D. Trombetta, A. Reza Mazaheri, M. Coleman, A. Olds, and S. Hancock. Heart flight test overview. *IPPW-9*, 2012.